


# Genome-wide identification and expression analysis of GDSL-type esterases/lipases (GELP) gene family in apple (*Malus × domestica* Borkh.)

Ru-Xue Sha<sup>1</sup>, Zi-Quan Feng<sup>1</sup>, Joy Xin Yue Zhai<sup>1,2</sup>, Tong Li<sup>1</sup>, Yun-Shuo Tian<sup>1</sup>, Hui-Min Lyu<sup>1</sup>, Han Jiang<sup>1</sup> , Shang Wu<sup>1</sup>, Ya-Li Zhang<sup>1\*</sup> and Yuan-Yuan Li<sup>1\*</sup>

<sup>1</sup> National Research Center for Apple Engineering and Technology, Shandong Collaborative Innovation Center of Fruit & Vegetable Quality and Efficient Production, College of Horticulture Science and Engineering, Shandong Agricultural University, Tai'an, Shandong 271018, China

<sup>2</sup> Shandong Experimental High School, Jinan, Shandong 250001, China

\* Correspondence: [ylzhang0522@163.com](mailto:ylzhang0522@163.com) (Zhang YL); [liy0912@163.com](mailto:liy0912@163.com) (Li YY)

## Abstract

The GDSL-type esterase/lipase family plays a crucial role in regulating plant growth and development, modulating responses to abiotic stresses, activating pathogen defense mechanisms, and governing lipid metabolism pathways. In this study, a comprehensive genome-wide analysis using integrated *BLASTP* and *HMMSEARCH* strategies identified 38 *MdGELP* genes in apple, which were mapped to 14 chromosomes. Phylogenetic analysis classified these genes into three major clades (A, B, and C). Multiple sequence alignment, combined with analyses of conserved domains and motifs, revealed a high degree of sequence conservation among *MdGELP* proteins. Promoter cis-acting element analysis uncovered diverse regulatory motifs, while gene duplication analysis indicated that segmental and tandem duplications were the primary evolutionary forces driving the expansion of the *GELP* family in apple. Collinearity analysis further highlighted significant homology between *MdGELPs* and *AtGELPs*. Quantitative expression assays revealed tissue-specific expression patterns, with *MdGELPs* showing preferential expression in leaves and flowers. Expression profiling under abiotic stresses (ABA, low-temperature, and salt) demonstrated their positive responsiveness to environmental challenges. This study not only establishes a theoretical foundation for exploring the biological functions of *MdGELPs* but also provides critical insights for future research in this field.

**Citation:** Sha RX, Feng ZQ, Zhai JXY, Li T, Tian YS, et al. 2026. Genome-wide identification and expression analysis of GDSL-type esterases/lipases (GELP) gene family in apple (*Malus × domestica* Borkh.). *Fruit Research* 6: e014 <https://doi.org/10.48130/frures-0026-0004>

## Introduction

The plant cuticle is an extracellular lipid structure deposited on the surface of terrestrial plants that seals off aerial organs and protects them from biotic and abiotic stresses. It is composed of a cutin polymer matrix and wax, which are produced and secreted by epidermal cells<sup>[1]</sup>. *GDSL* genes are essential for wax biosynthesis and the formation of stomatal cutin protrusions. As a class of hydrolases with broad substrate specificity, *GDSL* genes are widely distributed across various organisms and exhibit both esterases and lipase activities. For the sake of consistency, they will be collectively referred to as *GDSL* lipases hereafter. Mutations in *GDSL* lipase genes leads to a significant reduction in leaf wax synthesis and impaired stomatal closure, thereby increasing epidermal permeability reducing the transpiration rate<sup>[2]</sup>. Classified as a distinct subfamily from classical lipolytic enzymes, *GDSL* lipases (*GELPs*) are characterized by a conserved G × S × G motif and contain four conserved amino acid residues—serine (S), glycine (G), asparagine (N), and histidine (H)—which are located within at least four conserved structural domains. Consequently, *GELPs* are also known as SGNH lipase<sup>[3,4]</sup>. Unlike other lipases, *GELPs* can undergo conformational changes in response to different substrates through the an induced-fit mechanism<sup>[5,6]</sup>, enabling them to exhibit broad catalytic versatility and hydrolyze a wide range of substrates, including thioesters, aryl esters, phospholipids, and amino acids<sup>[7]</sup>.

*GELPs* are widely distributed in microorganisms, animals, and plants, where they play crucial roles in growth, development, and stress responses. However, research on plant *GELPs* began relatively late<sup>[8,9]</sup>. In 1995, Upton & Buckley first reported a *GELP* in *Aeromonas*

*hydrophila*, and named it based on its conserved structural domain characteristics (pfam PF00657)<sup>[7]</sup>. With the development of genomics and bioinformatics, a large number of *GELPs* have been identified in an increasing number of plants species. For instance, the model plant *Arabidopsis thaliana* harbors 105 members<sup>[10]</sup>, of which *Oryza sativa* contains 114 members<sup>[11]</sup>. *Pyrus spp.* has 113 members<sup>[12]</sup>. In the genomes of other sequenced species, such as the grain crops sorghum and maize<sup>[13,14]</sup>, there are 130 and 53 *GELP* members. Oilseed crops like soybean and sunflower have 194 and eight members, respectively<sup>[15]</sup>. *Ricinus communis* contains 96 *GELPs* members<sup>[16]</sup>. Through comparative analysis of the amino acid sequences of 604 *GELP* genes encoded by different terrestrial plants, it was found that members of the plant *GELP* family form three subfamilies (subfamily A, B, and C) in the phylogenetic tree, each containing *GELP* genes from different plant species<sup>[13]</sup>.

In recent years, the biological functions of *GELP* family members have been gradually elucidated. Several *GELPs* have been shown to participate in plant growth, development, and organ morphogenesis<sup>[17]</sup>. For example, the *Arabidopsis AtGELP* gene *AtEXL6* is involved in pollen development<sup>[18]</sup>. *AtOSP1* (occlusion of stomatal pore 1), an endoplasmic reticulum and lipid-localized *GELP*, plays a role in early wax biosynthesis and stomatal epidermal wall formation<sup>[2]</sup>. *AtGELP7* is a plasma membrane-localized protein that enhances saccharification efficiency<sup>[19]</sup>. The expression of many plant *GELP* genes can be induced by pathogens, hormones such as salicylic acid, ethylene, and jasmonic acid, as well as abiotic stress factors, suggesting their potential involvement in plant disease resistance and stress responses. For example, *AmGDSL1* is most

highly expressed in leaves, and is induced by drought stress, with its expression level showing a positive regulatory trend as stress duration increases<sup>[20]</sup>. Overexpression of longan *DIGDSL57* activates the antioxidant system and contributes to the high-temperature stress response<sup>[21]</sup>. Cosuppression of *AtGELP22* and *AtGELP23* enhances drought resistance by regulating the ABA-mediated signaling pathway<sup>[22]</sup>. Furthermore, *GELPs* are widely involved in the synthesis of plant secondary metabolites and fatty acid metabolism in oilseeds, and can catalyze the formation of lutein esters<sup>[13]</sup>. When the cotton *GELP* gene *GhGL1* was transferred into *Brassica napus*, seed oil content increased by 8.68%<sup>[23]</sup>. A rapid decline in *GELP* gene expression in Shatian grapefruit results in impaired intracellular ester metabolism<sup>[24]</sup>.

With the exception of a 2024 study on the molecular mechanism by which the apple lipase *MdGELP1* inhibits anthracnose infection<sup>[25]</sup>, research on *MdGELPs* remains limited. As the most economically valuable cultivated fruit tree in the Rosaceae family, apple (*Malus domestica* Borkh.) is widely grown in temperate regions worldwide, and ranks first globally in both production and cultivation area. Apple wax is a critical component of the fruit cuticle, playing an essential role in apple development, storage, and adaptation to environmental stress. The wax covering the apple surface directly determines its appearance quality and market value<sup>[26]</sup>. In this study, we used bioinformatics approaches to characterize the genome-wide members of the *MdGELPs* family, including their gene and protein structures. Additionally, we employed fluorescence qRT-PCR to analyze the tissue-specific expression of representative *MdGELPs* gene and investigated changes in their expression patterns under low-temperature, drought, and salt stresses. These findings provide a foundation for further exploring the regulatory mechanisms of wax synthesis and stress response in apple.

## Materials and methods

The experiment was conducted from January 2025 to June 2025 at Shandong Agricultural University.

### Plant materials and treatments

Two apple materials were selected for this study. Twenty-year-old 'Royal Gala' apple trees, planted at the Horticultural Experimental Station of Shandong Agricultural University (Tai'an, Shandong, China), were used to collect roots, young stems, leaves, flowers, and pericarp, and pulp tissues separately (130 d after flowering). All tissue samples were immediately snap-frozen in liquid nitrogen after collection and stored at  $-80^{\circ}\text{C}$  in an ultra-low-temperature refrigerator for subsequent tissue expression analysis. *Malus hupehensis* seedlings that had been cultured under laboratory conditions for approximately 4 months and exhibited uniform growth were selected for abiotic stress analysis. Three experimental treatments were applied to the *M. hupehensis* seedlings, with three biological replicates per treatment. For ABA treatment, three seedlings were transferred to a hydroponic system containing 10  $\mu\text{M}$  abscisic acid (ABA), and whole-plant samples were collected at 1, 2, 3, 6, 12, 24, and 48 h after treatment. For low-temperature stress treatment, three seedlings were incubated in a  $4^{\circ}\text{C}$  light incubator, and whole plants were sampled at 0, 1, 2, 3, 6, 12, 24, and 48 h after treatment. For salt stress treatment, three seedlings were incubated in a hydroponic system containing 150 mM NaCl, and whole plants were sampled at 1, 2, 3, 6, 12, 24, and 48 h after treatment. All samples from the three treatments were quickly frozen in liquid nitrogen and stored at  $-80^{\circ}\text{C}$  for subsequent abiotic stress expression analysis.

## Identification of the *MdGELPs* genes in apple

To identify *MdGELP* family members across the entire *Malus domestica* genome, we first downloaded 105 AtGELP protein sequences from the TAIR database (<https://arabidopsis.org>)<sup>[10]</sup>. Sequences shorter than 300 amino acids (aa), or longer than 350 aa, were filtered out, leaving 16 AtGELP protein sequences that were used as query sequences. A local BLASTP search was performed against the complete apple protein sequence library with an E-value threshold of  $1e-5$ . The *M. domestica* whole-genome sequence and GFF3 genome annotation data were retrieved from the Genome Database for Rosaceae (GDR, <https://rosaceae.org>). Additionally, the GDSL conserved domain (PF00657) file was downloaded from the Pfam database (<https://pfam.xfam.org>), and an HMMSEARCH was conducted with an E-value cutoff of  $1e-5$ . The candidate *MdGELP* proteins obtained through these two approaches were deduplicated and integrated using TBtools<sup>[27]</sup>. Subsequent domain confirmation via NCBI Batch CD-Search led to the identification of 38 *MdGELP* family members, which were designated as *MdGELP1* to *MdGELP38*.

### Analysis of *MdGELP* proteins Physicochemical properties of proteins

The molecular weight (MW), isoelectric point (pI), amino acid (aa) length, and other physicochemical properties of the 38 *MdGELP* proteins were calculated using the Phylogenetics plugin in TBtools.

### Multiple sequence alignment and conserved domain analysis

Multiple sequence alignment of the 38 *MdGELP* protein sequences was performed using DNAMAN (<https://dnaman.software.informer.com>) with default parameters, and the alignment results were visualized via the online tool WebLogo (<https://weblogo.berkeley.edu/logo.cgi>). Conserved domains of *MdGELP* proteins were analyzed using the online Batch CD-Search tool provided by the National Center for Biotechnology Information (NCBI), and the results were visualized with TBtools.

### Phylogenetic analysis

Using the previously obtained 16 AtGELP and 38 *MdGELP* protein sequences, a phylogenetic tree was constructed with MEGA7 using the neighbor-joining (NJ) method, and 1,000 bootstrap replications for validation. The phylogenetic tree was optimized and visualized using the online software Evolview (<https://evolgenius.info/evolview-v2/#login>).

### Conserved motif analysis

Conserved motif analysis was performed using the 'Simple MEME Wrapper' plugin in TBtools, with the number of motifs set to 8.

### Secondary and tertiary structure analysis

The secondary structures of the 38 *MdGELP* proteins were predicted using SOPMA ([https://npsa.lyon.inserm.fr/cgi-bin/npsa\\_automat.pl?page=/NPSA/npsa\\_sopma.html](https://npsa.lyon.inserm.fr/cgi-bin/npsa_automat.pl?page=/NPSA/npsa_sopma.html)). Homology modeling of the protein three-dimensional (3D) structures was conducted via the online tool SWISS-MODEL (<https://swissmodel.expasy.org>).

### Prediction of transmembrane domains, signal peptides, and phosphorylation sites

Transmembrane domains of the 38 *MdGELP* proteins were analyzed using TMHMM v.2.0 (<https://services.healthtech.dtu.dk/services/TMHMM-2.0>), while the presence of signal peptide structures in these protein sequences was annotated with SignalP 4.1 (<https://services.healthtech.dtu.dk/services/SignalP-4.1>). Phosphorylation sites of *MdGELP* proteins were predicted using the

online software NetPhos 3.1 (<https://services.healthtech.dtu.dk/services/NetPhos-3.1>).

### Subcellular localization prediction

Subcellular localization was predicted using the online tool CELLO (<https://cello.life.nctu.edu.tw>), with the organism set to 'Eukaryotes'.

### Protein interaction network and GO functional annotation (MdGELP to AtGELP homology mapping)

The protein interaction network of AtGELPs was predicted using the STRING database (<https://string-db.org>), with the organism specified as *Arabidopsis thaliana*. To further explore the functional homology of MdGELP proteins, we retrieved Gene Ontology (GO) term information for the 16 AtGELP proteins from the STRING database, followed by detailed bioinformatics processing and visual presentation of the data.

## Analysis of MdGELP genes

### Chromosomal localization

The chromosomal location information of the 38 MdGELP genes was extracted from the genome annotation file (gene\_models\_20170612.gff3), and submitted to TBtools for visualization of gene chromosomal distribution.

### Gene structure (exon-intron) analysis

Using the gene GFF annotation data, the exon-intron structures of the 38 MdGELP genes were visualized with TBtools.

### Analysis of MdGELP gene promoter cis-acting elements

The 2,000 bp upstream fragment of the translation start site (ATG) in the apple genome was defined as the promoter region. Promoter sequences of the 38 MdGELP genes were submitted to PlantCARE (<https://bioinformatics.psb.ugent.be/webtools/plantcare/html/>), and cis-acting elements were identified using default parameters. The results were visualized via TBtools.

### Intraspecific and interspecific collinearity analysis

To explore genetic homology across plant species, genome, and annotation files of *Arabidopsis thaliana* and *Oryza sativa* were downloaded from the NCBI database. Collinearity analysis was performed using the MScanX plugin in TBtools, and the non-synonymous substitution (Ka)/synonymous substitution (Ks) ratios of gene pairs were calculated using the Simple Ka/Ks Calculator (NG) plugin in TBtools.

### Analysis of MdGELP expression patterns

Total RNA was extracted from different tissues (roots, stems, leaves, flowers, pericarp, and pulp) of 'Royal Gala' apple trees, as well as from *Malus hupehensis* seedlings sampled at various time points under ABA, low-temperature, and salt stress treatments, using an RNA extraction kit (R2060; Beijing Solarbio Science & Technology Co., Ltd, Beijing, China). RNA concentration and purity were determined using a Thermo NanoDrop 2000 spectrophotometer. Complementary DNA (cDNA) was synthesized via reverse transcription using a commercial kit (Beijing Solarbio Science & Technology Co., Ltd, Beijing, China), followed by quantitative real-time PCR (qRT-PCR) analysis performed on a QuantStudio 7 Flex system. Gene-specific primers were designed using Primer3Plus (<https://primer3plus.com>), and their specificity was verified via NCBI Primer-BLAST (<https://blast.ncbi.nlm.nih.gov/Blast.cgi>). All primers used in this study are listed in Table 1, with 18S rRNA serving as the internal reference gene for apple. Relative gene expression levels were calculated using the  $2^{-\Delta\Delta C_t}$  method.

## Results

### Genome-wide identification, physicochemical properties, and subcellular localization of MdGELPs

A total of 38 MdGELP genes were identified in the apple (*Malus domestica*) genome and designated as MdGELP1 to MdGELP38. The amino acid lengths of the encoded proteins ranged from 337 (MdGELP36) to 419 (MdGELP21), with molecular weights (MW) of 36.76–46.37 kDa, and isoelectric points (pI) of 4.59–9.12. Most proteins (34 out of 38, 89.5%) exhibited a stability index < 40, indicating good *in vitro* stability. Subcellular localization prediction revealed that 21 members (55.3%) were localized to the plasma membrane, 14 (36.8%) to the extracellular space, and the remaining three (MdGELP10, MdGELP15, MdGELP29) to the cytoplasm or vacuoles. These results suggest that MdGELPs may exert diverse functional roles in membrane transport, secretion, and metabolic regulation (Table 2).

### Phylogenetic tree and conserved region analysis

Phylogenetic analysis of 38 MdGELP and 16 AtGELP proteins was performed using the neighbor-joining (NJ) method with 1,000 bootstrap replicates. The resulting tree divided the family into three major clades (Clade A, B, and C), containing 25, 28, and one member, respectively. Clade B was the largest, comprising 13 MdGELPs and 15 AtGELPs, while Clade C contained only AtGELP15. Both Clade A and Clade B could be further subdivided into two subclades. Several orthologous relationships were identified, including between MdGELP27 and AtGELP9 (Fig. 1a). Multiple sequence alignment confirmed high conservation of key motifs among these proteins (Fig. 1b). Motif analysis using MEME identified eight conserved motifs, with Motif 1, Motif 3, and Motif 4 present in all members (Fig. 1c). Notably, all MdGELP proteins in Clade B contained Motif 8, suggesting that this motif may contribute to their shared functional characteristics. Conserved domain analysis revealed the presence of both SGNH and GDSL domains in all MdGELP proteins (Fig. 1d). The vast majority of Clade B proteins contained only the SGNH domain. To further explore similarities and differences among MdGELPs at the nucleic acid level, we visualized their exon-intron structures (Fig. 1e). The results showed that most MdGELPs (28/38) contained either 3 or 5 exons, with MdGELP36 having the highest (7 exons). The

**Table 1.** Real-time fluorescence quantitative PCR primers for relative expression of MdGELPs.

Gene	Forward primer (5'-3')	Reverse primer (5'-3')
MdGELP2	GACTTTGATGAAGCGTTGAGGAG	GAATGAACGACCCGAGTCTTTT
MdGELP3	AAATAGGGATTGCTCCGAGACTG	TAACGAGTACACAGGACGCTAAC
MdGELP6	TGCTAGATCTCGCCAATTCTCTC	CGACTAGTTGTGGTTGAAC AAG
MdGELP8	CTTTGAAGGGGGAGTGAATTTCTG	CTCCCATGAGAATTAGAGA GCCC
MdGELP14	GTTACAACAATGTGGCCTTGAG	GTAGCCCATTTCAAACATCC CAG
MdGELP18	CCAAAACACAGTGTCTCAAGTGG	GTTGACCCTAATCGTGAATG AGC
MdGELP26	ATCTATATGCACTGGGAGCAAGG	AGCGGTTGGTAGATATCAA GGAC
MdGELP28	GCAGCAGGTATTCTGATGAATC	GGCGGCTAGTTGAGTATAA CCTT
MdGELP31	GGTGATATTGTCCAGATGCATGC	GCCGGTATCAACAATCGAAT CTC

**Table 2.** Physical and chemical properties of MdGELPs.

Gene name	Gene ID	Number of amino acid	Molecular weight (Da)	Theoretical pI	Instability index	Aliphatic index	Grand average of hydropathicity	Subcellular localization prediction
MdGELP1	MD00G1093600	365	40,038.95	6.72	26.17	78.6	-0.168	Extracellular
MdGELP2	MD01G1156400	361	39,941.92	9.12	40.29	88.31	-0.106	Extracellular
MdGELP3	MD02G1126900	366	40,088.96	8.42	37.79	96.69	0.029	PlasmaMembrane
MdGELP4	MD02G1127000	359	39,242	8.95	34	92.56	0.009	PlasmaMembrane
MdGELP5	MD02G1127100	349	38,230.71	8.67	33.06	96.07	0.02	PlasmaMembrane
MdGELP6	MD04G1234300	362	39,890.29	5.26	31.61	92.18	0.002	PlasmaMembrane
MdGELP7	MD05G1293600	330	36,765.6	7.54	38.02	84.52	-0.125	PlasmaMembrane
MdGELP8	MD05G1304000	376	41,660.12	4.59	44.12	86.14	-0.002	PlasmaMembrane
MdGELP9	MD07G1225100	361	39,543.43	8.13	37.94	91.27	0.025	Extracellular
MdGELP10	MD08G1009700	381	41,885.18	6.82	31.83	93.1	-0.02	Cytoplasmic
MdGELP11	MD08G1009800	380	41,341.35	5.03	40.88	95.34	0.099	PlasmaMembrane
MdGELP12	MD08G1215700	377	41,683.24	9.03	33.69	81.78	-0.102	PlasmaMembrane
MdGELP13	MD09G1116400	350	39,094.76	8.34	34.53	86.11	-0.052	PlasmaMembrane
MdGELP14	MD09G1116500	349	38,651.25	8.34	35.09	83.87	-0.045	PlasmaMembrane
MdGELP15	MD09G1116600	350	39,579.22	5.54	28.05	84.69	-0.159	Vacuole
MdGELP16	MD09G1148500	349	39,053.98	6.35	30.2	88.88	-0.038	PlasmaMembrane
MdGELP17	MD09G1199700	388	41,943.68	8.88	25.24	85.31	-0.036	Extracellular
MdGELP18	MD10G1270600	366	40,134.91	4.95	24.81	82.1	-0.151	Extracellular
MdGELP19	MD10G1270700	368	40,247.69	5.65	22.19	84.84	-0.149	Extracellular
MdGELP20	MD10G1270800	362	39,373.54	5.59	34.47	84.09	-0.047	Extracellular
MdGELP21	MD10G1270900	419	46,368.76	8.68	30.98	76.09	-0.252	Extracellular
MdGELP22	MD10G1283000	367	40,296.18	8.52	36.87	85.64	0.028	Extracellular
MdGELP23	MD10G1283400	371	41,088.41	4.65	44.34	87.82	-0.019	PlasmaMembrane
MdGELP24	MD10G1286100	356	38,944.27	8.5	25.47	97.47	0.092	PlasmaMembrane
MdGELP25	MD11G1058600	377	41,838.96	6.6	37.12	89.71	-0.105	Extracellular
MdGELP26	MD11G1153800	354	38,492.65	5.41	28.38	92.37	0.056	Extracellular
MdGELP27	MD11G1210200	349	39,157.06	7.51	26.79	89.66	-0.003	PlasmaMembrane
MdGELP28	MD12G1049900	369	40,378.84	6.97	32.11	90.38	0.038	Extracellular
MdGELP29	MD15G1008700	368	41,202.58	8.89	28.53	89.73	-0.111	Cytoplasmic
MdGELP30	MD15G1008800	379	42,085.47	6.88	30.74	94.59	-0.005	PlasmaMembrane
MdGELP31	MD15G1008900	400	44,117.95	7.49	30.63	100.15	0.075	PlasmaMembrane
MdGELP32	MD15G1009100	379	42,003.4	6.02	31.44	97.18	0	PlasmaMembrane
MdGELP33	MD15G1009500	370	40,696.89	6.87	37.02	93.73	0.076	PlasmaMembrane
MdGELP34	MD15G1009600	362	39,653.51	4.83	22.11	95.86	0.071	PlasmaMembrane
MdGELP35	MD15G1241700	373	41,369.63	9.1	32.72	88.53	-0.014	PlasmaMembrane
MdGELP36	MD15G1241800	337	37,835.66	5.63	29.19	101.72	0.249	PlasmaMembrane
MdGELP37	MD15G1400200	391	42,794.36	5.29	33.22	84.35	-0.137	Extracellular
MdGELP38	MD17G1180300	357	38,251.51	6.5	22.84	91.06	0.099	Extracellular

relatively conserved gene structures suggest similar regulatory mechanisms, while variations in intron number (2–6)<sup>[16]</sup> may reflect evolutionary divergence through intron gain/loss events<sup>[28]</sup>.

### Characteristics and structural predictions of MdGELP proteins

Secondary structure prediction revealed that all MdGELP proteins are primarily composed of  $\alpha$ -helices and random coils, with minimal  $\beta$ -turns (Fig. 2a). Tertiary structure modeling showed highly similar three-dimensional (3D) conformations among family members, further supporting functional conservation (Fig. 2b). TMHMM analysis identified 13 MdGELPs (MdGELP2/8/9/12/17/18/20/22/26/28/33/36/38) containing a single transmembrane domain, suggesting potential roles in membrane-associated signaling (Fig. 2c). Signal peptide prediction indicated that 23 proteins harbor secretory signals, with the cleavage site of MdGELP37 localized between amino acids 30 and 31 (Fig. 2d). Protein phosphorylation plays a core regulatory role in plant growth and development, environmental adaptability, and signal transduction<sup>[29]</sup>. Phosphorylation site analysis detected 1,283 total sites, predominantly on serine (49.26%), threonine (27.83%), and tyrosine (22.91%) residues, with MdGELP35 protein exhibiting the highest phosphorylation site

density (Fig. 2e). Collectively, these results indicate that MdGELP proteins are functionally conserved, with some members having transmembrane properties, and may be regulated through phosphorylation modifications.

### Chromosomal localization and collinearity analysis

We conducted a detailed analysis of the chromosomal localization and gene structural features of the 38 MdGELP genes. These genes were mapped to 14 apple chromosomes. Notably, chromosome 15 exhibited the highest gene density, harboring 10 MdGELP genes (26.3% of the total) (Fig. 3a). MdGELP1 was located on an unanchored scaffold, indicating that it has not yet been assigned to a specific chromosome in the current genome assembly, which reflects limitations in the current annotation. Genes such as MdGELP18–21 were closely clustered on the same chromosome, suggesting potential tandem duplication events during evolution. Tandem duplication, a key mechanism of gene amplification, increases gene copy numbers and may enhance adaptive potential. To clarify the phylogenetic relationships among MdGELP family genes, we performed an intraspecific collinearity analysis (Fig. 3a). The analysis identified seven tandem duplication events,

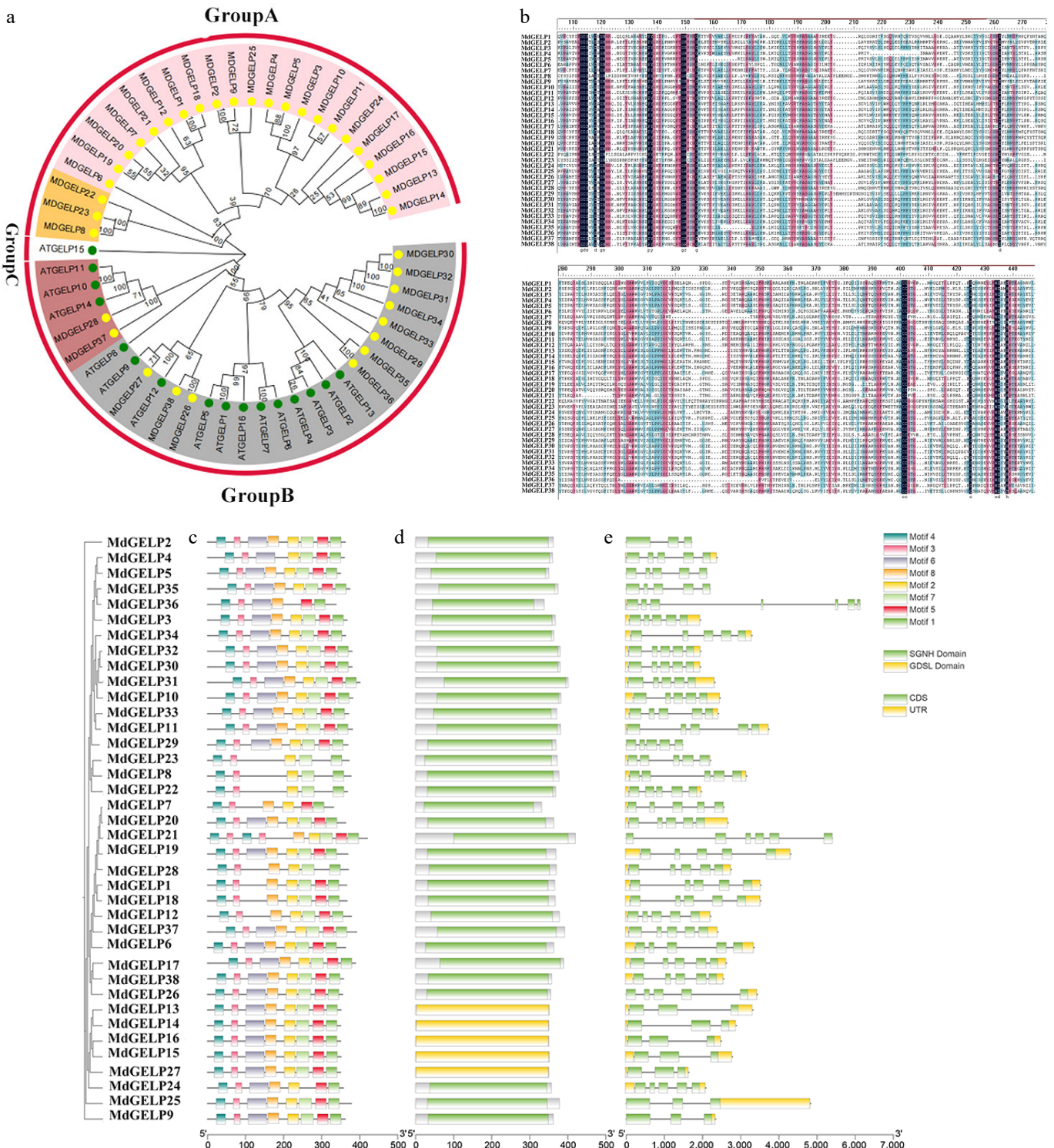


**Fig. 1** Phylogenetic tree and conserved region analysis. (a) Phylogenetic tree of GELP proteins from *Malus domestica* and *Arabidopsis thaliana*. (b) Multiple sequence alignment of MdGELP family protein. (c) Distribution of conserved motifs MdGELP family proteins. (d) Distribution of conserved domains in MdGELP family proteins. (e) Gene structure analysis of MdGELPs.

and 11 segmental duplication events within the family. Segmental duplication, which may arise from whole-genome duplication or large-scale chromosomal recombination, occurred 1.57 times more frequently than tandem duplication. Synteny analysis is a key strategy in comparative genomics for evaluating molecular evolutionary relationships between species<sup>[30]</sup>. We performed interspecific collinearity analysis among *Arabidopsis thaliana*, apple (*Malus*

*domestica*), and rice (*Oryza sativa*). The results showed more collinear gene pairs between apple and Arabidopsis than between apple and rice, indicating a closer evolutionary relationship and higher functional conservation between apple and Arabidopsis (Fig. 3b). This finding enhances our understanding of plant genome evolution and facilitates the prediction of MdGELP biological functions. We calculated the Ka/Ks ratios of all paralogous gene pairs.

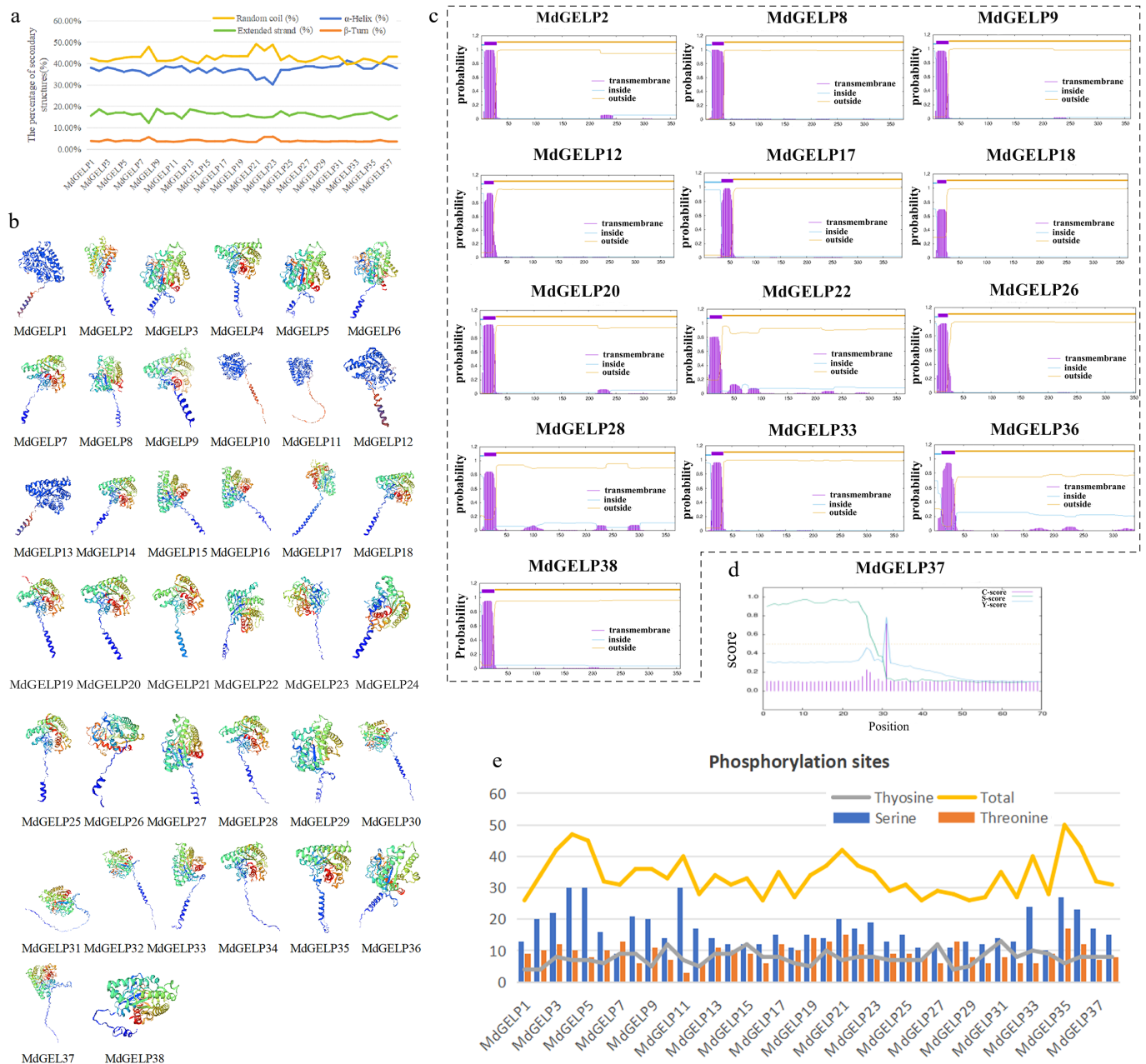


**Fig. 2** Characteristics and structural prediction of MdGELP protein. (a) Secondary structure prediction of MdGELP proteins; the four colors represent different secondary structure elements, respectively. (b) Tertiary structure prediction of MdGELP proteins; the four colors represent different subunits, respectively. (c) Transmembrane domain prediction of MdGELP proteins. Gene names are listed above the plot. In the plot, the x-axis represents protein sequence length and the y-axis represents the probability of transmembrane regions. (d) Signal peptide prediction for MdGELP37. (e) Prediction of phosphorylation site distribution in MdGELP amino acid sequences.

The results showed that the vast majority of values were significantly less than 1, indicating that the *MdGELP* family has been primarily influenced by purifying selection during evolution (Supplementary Table S1). This analysis provides key evolutionary evidence supporting the functional conservation of the family.

### Promoter cis-acting elements, tissue expression patterns, and responses to abiotic stress

Using PlantCARE, we predicted and analyzed cis-acting elements in the 2,000 bp promoter regions of the 38 *MdGELP* genes (Fig. 4a). These elements were associated with stress responses (e.g., anaerobic conditions, low temperature, and drought, etc.), phytohormone

regulation (e.g., abscisic acid and auxin), and growth-related processes, and were classified into 18 functional categories. Among all *MdGELP* promoters, that of *MdGELP37* contained the highest number of elements (18). To investigate the tissue-specific expression patterns of *MdGELP* family genes, we performed qRT-PCR analysis on nine representative *MdGELPs*. The results showed that these genes are broadly expressed across different tissues but exhibit distinct expression profiles in roots, stems, leaves, flowers, pericarp, and flesh. Most of the nine genes were more highly expressed in leaves and flowers (Fig. 4b, Supplementary Table S2), suggesting potential roles in the development or function of these organs. Further studies are needed to determine whether other

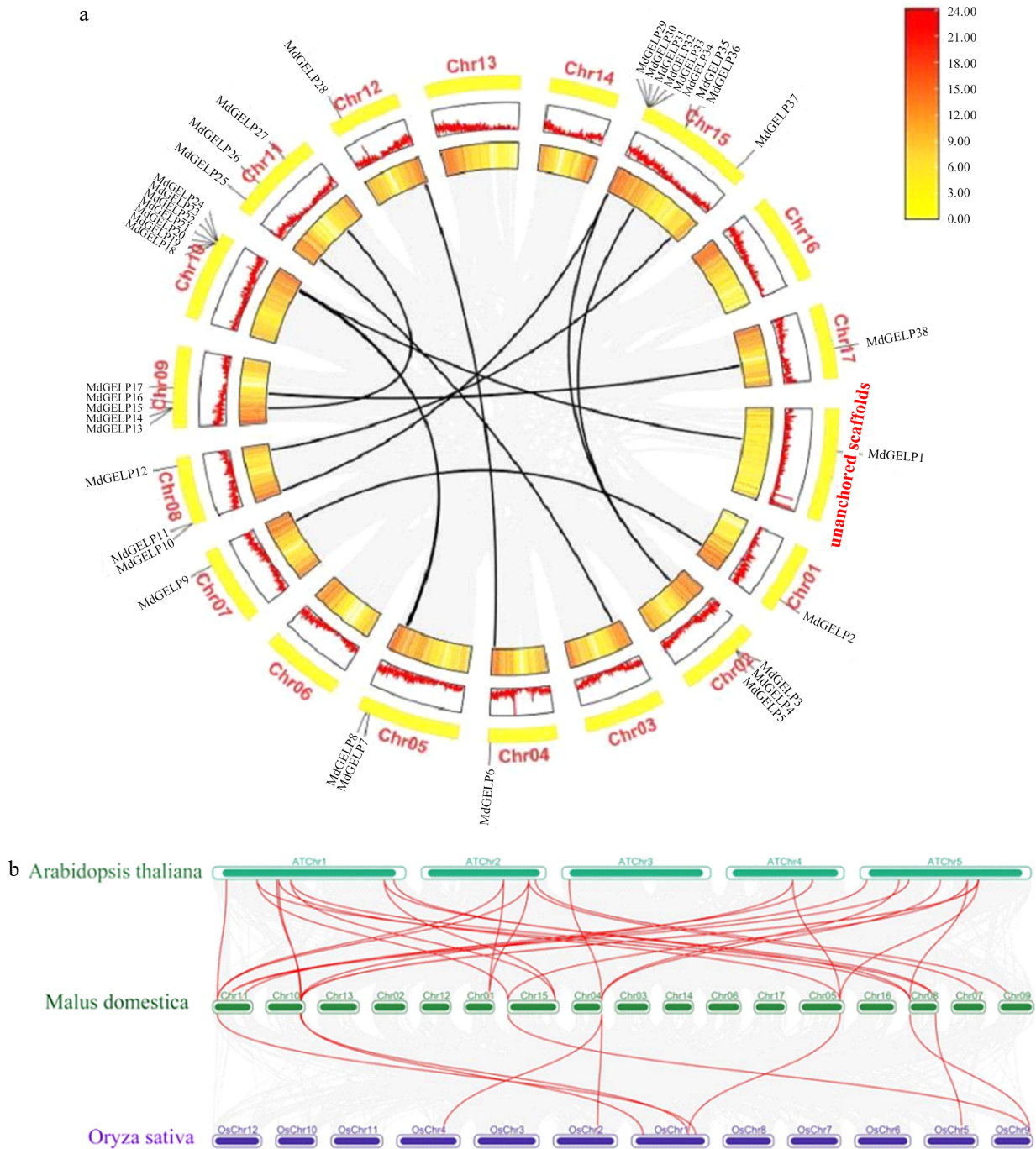


**Fig. 3** Chromosomal localization and collinearity analysis. (a) Chromosomal distribution of *MdGELPs* and tandem/fragment repetition, with *MdGELP1* located in unanchored scaffolds. (b) Collinearity analysis among apple, *Arabidopsis thaliana*, and rice. Dark green boxes represent the 17 apple chromosomes, green boxes represent the five *Arabidopsis thaliana* chromosomes, and purple boxes represent the 12 rice chromosomes. Red lines indicate homologous gene pairs.

family members share similar expression patterns. The observed tissue specificity is consistent with findings in soybean<sup>[15]</sup>.

Since abscisic acid (ABA) plays a crucial role in plant tolerance to abiotic stresses such as heavy metals, drought, and extreme temperatures<sup>[31]</sup>, we treated *Malus hupehensis* seedlings with ABA to examine *MdGELP* responses (Fig. 4c, Supplementary Table S3). Some genes, including *MdGELP2* and *MdGELP6*, were initially upregulated and then downregulated, with peak expression at 2-6 h post-treatment, while *MdGELP31* showed significant upregulation throughout the treatment period. Given that *GELPs* may be involved

in plant tolerance to low-temperature stress, we analyzed *MdGELP* expression under low-temperature conditions (Fig. 4d, Supplementary Table S3). Except for *MdGELP26*, *MdGELP28*, and *MdGELP31*, the other six genes showed a pattern of initial upregulation followed by downregulation as the duration of low-temperature stress increased. Previous research has suggested that *GELPs* may mediate plant responses to salt stress through osmotic regulation and phytohormone signaling<sup>[32]</sup>. We therefore analyzed *MdGELP* expression patterns under salt treatment (Fig. 4e, Supplementary Table S3). Most *MdGELPs*, including *MdGELP2* and *MdGELP3*, were upregulated.

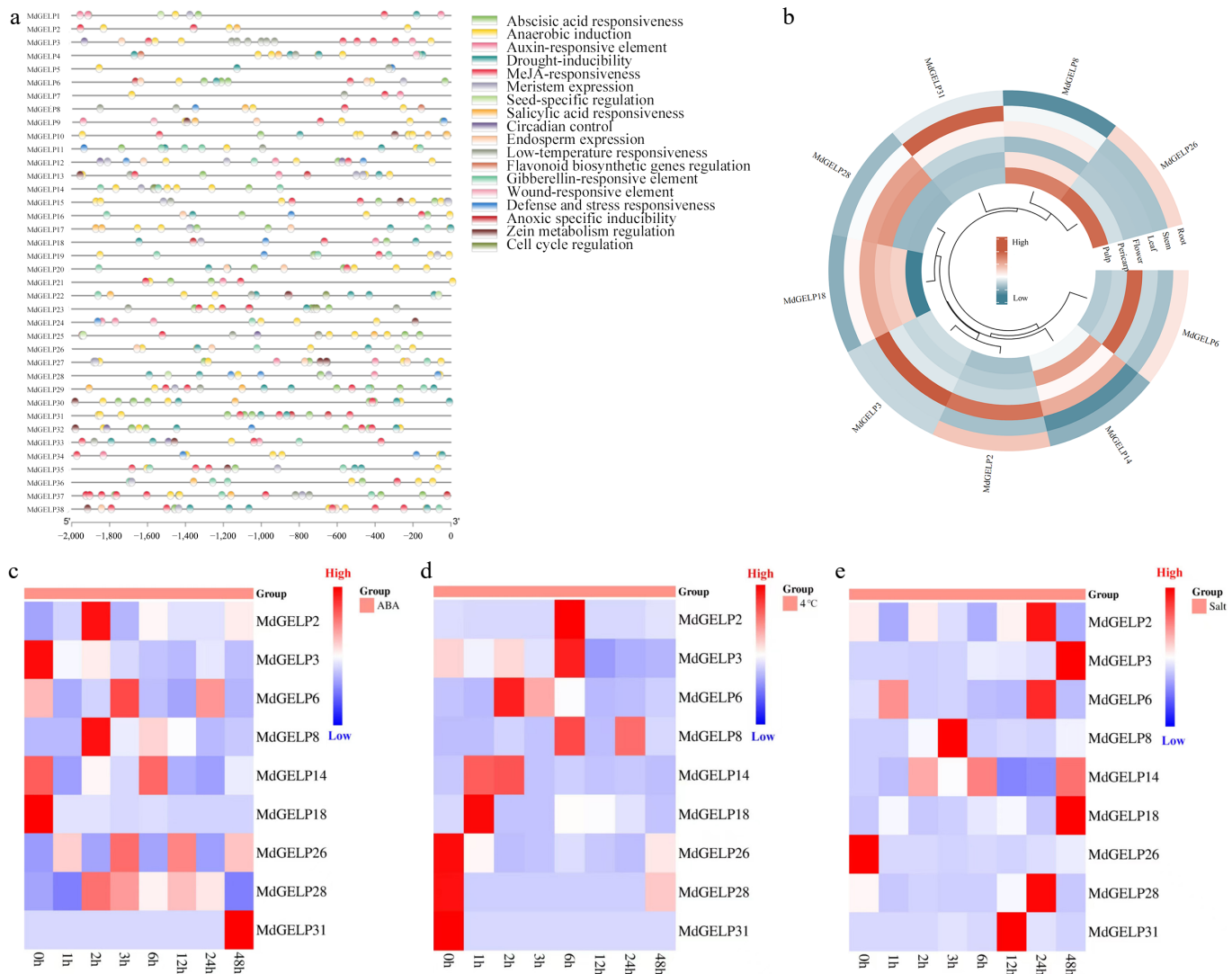


**Fig. 4** Promoter cis-acting element analysis and expression profiling. (a) Analysis of cis-acting elements in the promoter regions of *MdGELPs*. (b) Expression levels of *MdGELPs* in roots, stems, leaves, flowers, pericarp, and flesh as determined by qRT-PCR. (c) Relative expression under ABA treatment. (d) Relative expression under low-temperature stress. (e) Relative expression under salt stress.

*MdGELP8* showed an initial increase, followed by a decrease, with peak expression at 3 h.

### Protein interaction network and GO annotation

The STRING database was used to predict the protein interaction network of *AtGELPs*, revealing several key nodes such as GRP17, which is involved in pollen wall formation<sup>[33]</sup>(Fig. 5a, b). GO enrichment analysis categorized *AtGELPs* into three main functional groups: biological processes (e.g., lipid degradation, GO:0016042), molecular functions (e.g., lipase/hydrolase activity, GO:0016289/GO:0016788), and cellular components (e.g., extracellular region/extracellular space, GO:0005576/GO:0070505). These results support the conserved roles of GELP proteins in lipid metabolism and stress responses (Fig. 5c, Supplementary Table S4).

### Discussion

*GELPs* are a recently identified subfamily of lipolytic enzymes<sup>[10]</sup>. Although they play key roles in plant wax synthesis and stress responses<sup>[34]</sup>, their functions in apple (*Malus domestica* Borkh.)

remain largely unclear. In this study, we identified 38 *MdGELPs* containing both GDSL and SGNH domains. Bioinformatics analyses were used to characterize their gene and protein features, while expression patterns across different tissues and in response to ABA, low-temperature, and salt stress were investigated. These findings provide a foundation for understanding GELP function in apple and may be valuable for breeding stress-resilient crop varieties. Subcellular localization predictions revealed that *MdGELPs* predominantly accumulate in the extracellular matrix and cell membrane, consistent with previous reports<sup>[35]</sup>, suggesting that GELP genes may mediate signal transduction from the extracellular environment to the inside of the cell<sup>[16]</sup>. Additionally, some proteins were predicted to localize to the cytoplasm and vacuoles. Such differential subcellular distributions imply that *MdGELPs* may possess diverse biological functions.

As an evolutionary concept, homology is most reliably inferred through phylogenetic analysis<sup>[36]</sup>. Our phylogenetic results indicate that this gene family is widely distributed across species ranging from lower to higher plants. In this study, *MdGELP* proteins were classified into three groups (Fig. 1a), consistent with previous findings that terrestrial plant GELPs form three subfamilies<sup>[37]</sup>. Most

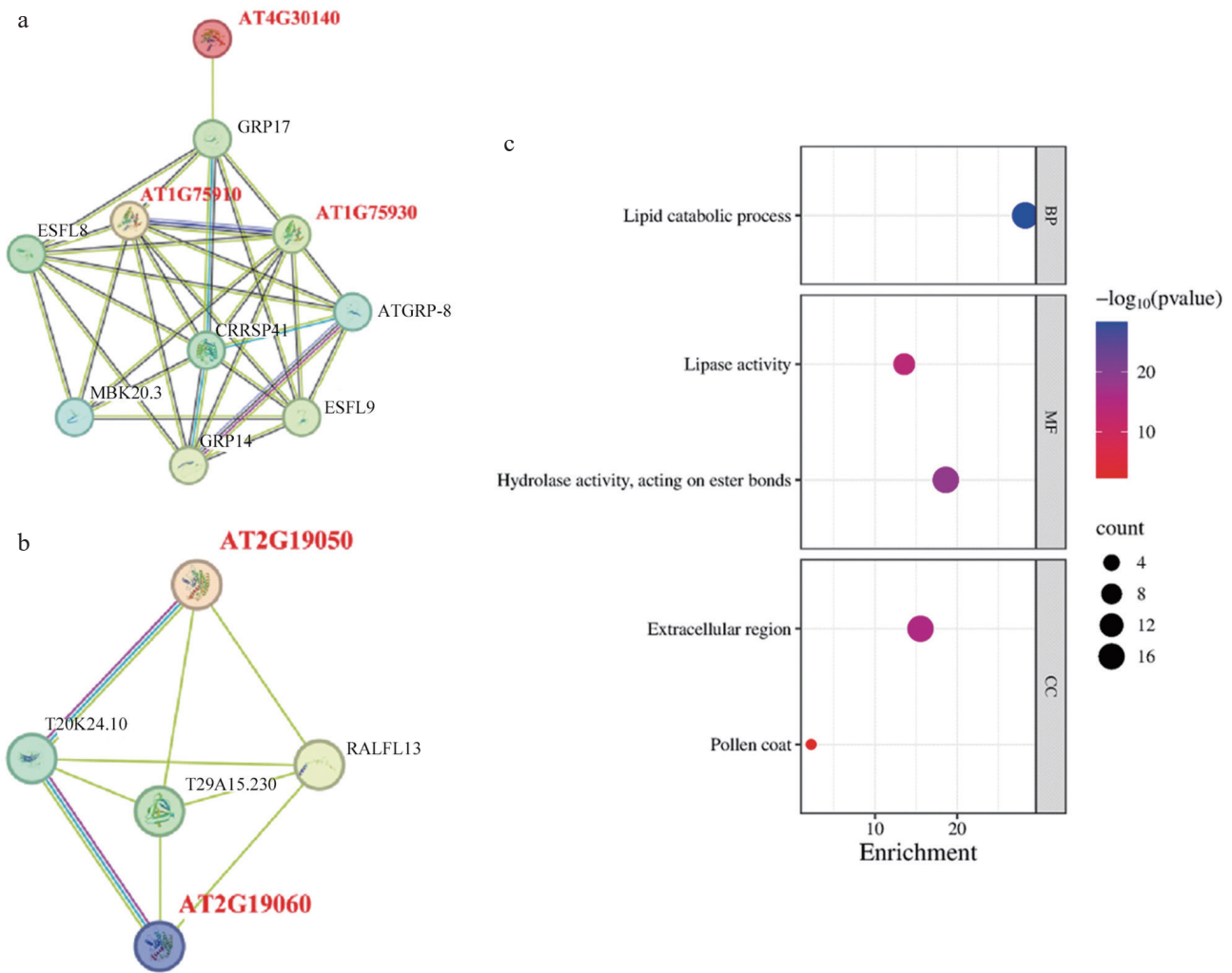


**Fig. 5** Protein interaction network and GO annotation. (a), (b) Prediction of the AtGELP protein interaction network. (c) GO enrichment analysis of AtGELP proteins. Bubble size indicates the number of genes, and color indicates the *p*-value.

*Arabidopsis thaliana* GELP genes contain four introns, which aligns with our results<sup>[37]</sup>. The intron number in the GELP family varies from 2 to 5 (Fig. 1e), likely due to intron gain events. Intron acquisition and loss are crucial processes in eukaryotic evolution<sup>[38,39]</sup>, contributing to differences in gene structure and functional divergence. Notably, *MdGELPs* exhibit highly similar gene structures and domain compositions, suggesting a conserved evolutionary trajectory. Collectively, this study provides important references for future functional research on the *MdGELP* family.

The expansion of gene families provides the foundation for functional diversification. Because of functional redundancy, multiple genes can be rapidly silenced or lost from duplicated genomes<sup>[40]</sup>. During plant evolution, increases in gene family size primarily occur through tandem duplication and segmental duplication events<sup>[41,42]</sup>. In *Arabidopsis*, approximately 44% (46/105) of GELPs form 16 tandem clusters on chromosomes, with 2–9 genes per cluster. In rice, about 47% (54/114) of *OsGELPs* are tightly clustered<sup>[15]</sup>. In apple, 68% (26/38) of *MdGELPs* exist as tandem repeats (Fig. 3a), highlighting tandem duplication as a major driver of family expansion. In addition, 11 segmental duplication events were detected in the apple genome. These findings are consistent with previous studies on GELP family evolution in terrestrial plants<sup>[37]</sup>. Collinearity analysis revealed that the number of collinear gene pairs between *MdGELPs* and *AtGELPs* is more than three times that between

*MdGELPs* and *OsGELPs* (Fig. 3b). Thus, functional knowledge of *AtGELPs* can serve as a valuable reference for inferring the potential functions of *MdGELPs*.

After family expansion, members may undergo functional differentiation, and diversity in transcriptional regulation is an important manifestation of this process. To explore this, we analyzed cis-acting elements in the promoter regions of *MdGELPs*. To elucidate the roles of *MdGELPs* in apple development, we identified diverse cis-acting elements in their promoters (Fig. 4a). These results indicate that *MdGELP* expression may be modulated by phytohormones and environmental stresses, consistent with previous studies in *Carya illinoensis*<sup>[43]</sup>. Hormone-related elements, including those responsive to abscisic acid (ABA), methyl jasmonate (MeJA), and gibberellin (GA), were detected in nearly all *MdGELP* promoter regions, suggesting that *MdGELPs* are involved in apple tissue development and growth. In our study, cis-acting elements related to seed-specific regulation, circadian rhythm, and endosperm expression were identified in the promoters of *MdGELP1*, *MdGELP3*, and *MdGELP6*. Analogously, *GER1* in rice is regulated by MeJA and light<sup>[44]</sup>. Furthermore, numerous anaerobic stress-associated elements were found, consistent with previous observations in *Carya illinoensis*<sup>[43]</sup>. Overall, the diverse cis-acting elements in *MdGELP* promoters imply that their expression is fine-tuned by

multiple environmental and endogenous signals, enabling *MdGELPs* to perform varied functions throughout apple development.

The presence of the aforementioned regulatory elements suggests that *MdGELPs* may exhibit tissue-specific expression patterns. We tested this hypothesis by analyzing the tissue expression profiles of selected *MdGELP* genes. Studies of *GELP* expression in different plant tissues have shown that these genes are widely distributed across nearly all examined organs. In soybean, *GmGELP22*, *GmGELP149*, and *GmGELP186* are highly transcribed in most tissues throughout the growth cycle<sup>[15]</sup>. In *Brassica napus*, the *GELP* family member *BnaLIP1* is expressed in roots, stems, leaves, flowers, pods, and flower buds<sup>[45]</sup>. Consistent with these findings, the nine *MdGELPs* examined in this study are expressed in roots, stems, leaves, flowers, pericarp, and flesh, but their expression levels vary significantly among tissues (Fig. 4b). From an evolutionary perspective, gene duplication often increases genetic diversity and can lead to gene loss, whereas duplicated genes that undergo functional differentiation tend to be retained by natural selection<sup>[46]</sup>. The results of this study are consistent with these concepts.

Finally, to investigate the potential role of *MdGELPs* in stress responses, we analyzed their expression under several abiotic stress conditions. Analysis of *MdGELP* expression profiles under ABA, low-temperature, and salt stress (Fig. 4c–e) showed that *MdGELP14* and *MdGELP18* were significantly downregulated during ABA and low-temperature treatments. In contrast, *MdGELP2*, *MdGELP3*, *MdGELP6*, *MdGELP14*, *MdGELP18*, *MdGELP28*, and *MdGELP31* were upregulated under salt stress. Notably, *MdGELP3* was significantly induced under both low-temperature and salt stress, indicating that it may act as a core regulatory factor in cross-stress responses. In particular, it exhibited a typical 'induction followed by inhibition' expression pattern under low-temperature stress. The promoter region of *MdGELP3* contains multiple elements related to low-temperature stress, which is consistent with its rapid induction during the early phase of low-temperature response (Fig. 4a). In addition, previous research has demonstrated that MeJA participates in plant defense responses against various abiotic stresses<sup>[47]</sup>. In tomato, for example, MeJA promotes abscisic acid (ABA) biosynthesis and plays a crucial role in low-temperature stress resistance<sup>[48]</sup>. The *MdGELP3* promoter region was predicted to contain an abundance of MeJA-responsive elements, suggesting that *MdGELP3* may integrate hormone signals to coordinate defense responses (Fig. 4a).

## Conclusions

Despite the importance of the *MdGELP* gene family, the functions of its members remain poorly understood in apple, with only a few genes having been characterized in any detail. In this study, we identified 38 *MdGELP* genes from the apple genome, and classified them into three distinct groups. Promoter analysis revealed numerous cis-acting elements associated with growth, abiotic stress responses, and phytohormone regulation. Tissue-specific expression profiling showed that *MdGELPs* preferentially accumulate in leaves and flowers. Under abiotic stresses—including ABA treatment, low temperature, and salt exposure—*MdGELPs* exhibited dynamic expression changes, highlighting their potential roles in stress adaptation. Comparative analysis revealed both conserved and divergent features in the protein structures and expression patterns of *MdGELPs*. While sharing several similarities, these genes also exhibit subtle differences, suggesting that they have both overlapping and distinct functions in mediating responses to abiotic stress.

## Ethical statements

Not applicable

## Author contributions

The authors confirm their contributions to the paper as follows: writing of original draft: Sha RX, Feng ZQ; formal analysis, methodology, and validation: Zhai JXY, Li T, Tian YS, Lyu HM, Jiang H, Wu S; supervision, resources, funding acquisition, writing – review and editing: Zhang YL, Li YY; made equal contributions to the article: Feng ZQ, Sha RX, Zhai JXY. All authors reviewed the results and approved the final version of the manuscript.

## Data availability

The datasets generated during and/or analyzed in the current study are available from the corresponding author on reasonable request.

## Acknowledgments

This work was supported by the National Key Research and Development Program (2023YFD2301000), the National Natural Science Foundation of China (32472705 and 32402536), Natural Science Foundation of Shandong Province (ZR2022JQ14), and Taishan Scholar Project.

## Conflict of interest

The authors declare that they have no conflict of interest.

**Supplementary information** accompanies this paper online at: <https://doi.org/10.48130/frures-0026-0004>.

## Dates

Received 5 November 2025; Revised 8 January 2026; Accepted 13 January 2026; Published online 14 April 2026

## References

- [1] Kunst L, Samuels L. 2009. Plant cuticles shine: advances in wax biosynthesis and export. *Current Opinion in Plant Biology* 12:721–727
- [2] Tang J, Yang X, Xiao C, Li J, Chen Y, et al. 2020. GDSL lipase occluded stomatal pore 1 is required for wax biosynthesis and stomatal cuticular ledge formation. *New Phytologist* 228:1880–1896
- [3] Akoh CC, Lee GC, Liaw YC, Huang TH, Shaw JF. 2004. GDSL family of serine esterases/lipases. *Progress in Lipid Research* 43:534–552
- [4] Brick DJ, Brumlik MJ, Buckley JT, Cao JX, Davies PC, et al. 1995. A new family of lipolytic plant enzymes with members in rice, arabidopsis and maize. *FEBS Letters* 377:475–480
- [5] Neves Petersen MT, Fojan P, Petersen SB. 2001. How do lipases and esterases work: the electrostatic contribution. *Journal of Biotechnology* 85:115–147
- [6] Huang YT, Liaw YC, Gorbatyuk VY, Huang TH. 2001. Backbone dynamics of *Escherichia coli* thioesterase/protease I: evidence of a flexible active-site environment for a serine protease. *Journal of Molecular Biology* 307:1075–1090
- [7] Upton C, Buckley JT. 1995. A new family of lipolytic enzymes? *Trends in Biochemical Sciences* 20:178–179
- [8] Li ZZ. 2014. *In Silico analysis of GDSL genes in Arabidopsis and brassica and the investigation on their function in seeds*. PhD. Thesis. Zhejiang University.

- [9] Yang D, He X, Li S, Liu J, Stabenow J, et al. 2019. Rv1075c of *Mycobacterium tuberculosis* is a GDSL-like esterase and is important for intracellular survival. *The Journal of Infectious Diseases* 220:677–686
- [10] Lai CP, Huang LM, Chen LO, Chan MT, Shaw JF. 2017. Genome-wide analysis of GDSL-type esterases/lipases in *Arabidopsis*. *Plant Molecular Biology* 95:181–197
- [11] Chepyshko H, Lai CP, Huang LM, Liu JH, Shaw JF. 2012. Multifunctionality and diversity of GDSL esterase/lipase gene family in rice (*Oryza sativa* L. *japonica*) genome: new insights from bioinformatics analysis. *BMC Genomics* 13:309
- [12] Zhang P, Zhang H, Du J, Qiao Y. 2022. Genome-wide identification and co-expression analysis of GDSL genes related to suberin formation during fruit russeting in pear. *Horticultural Plant Journal* 8:153–170
- [13] Volokita M, Rosilio-Brami T, Rivkin N, Zik M. 2011. Combining comparative sequence and genomic data to ascertain phylogenetic relationships and explore the evolution of the large GDSL-lipase family in land plants. *Molecular Biology and Evolution* 28:551–565
- [14] Zhang C, Ren W, Geng X, Li D, Wu H, et al. 2022. Genome-wide Identification and Expressions of Banana GDSL Lipase Gene Family. *Fujian Journal of Agricultural Sciences* 37:1415–1429 (in Chinese)
- [15] Su HG, Zhang XH, Wang TT, Wei WL, Wang YX, et al. 2020. Genome-wide identification, evolution, and expression of GDSL-type esterase/lipase gene family in soybean. *Frontiers in Plant Science* 11:726
- [16] de Almeida CP, Barbosa RR, Ferraz CG, de Castro RD, Ribeiro PR. 2024. Genome-wide identification of the GDSL-type esterase/lipase protein (GELP) gene family in *Ricinus communis* and its transcriptional regulation during germination and seedling establishment under different abiotic stresses. *Plant Physiology and Biochemistry* 214:108939
- [17] Takahashi K, Shimada T, Kondo M, Tamai A, Mori M, et al. 2010. Ectopic expression of an esterase, which is a candidate for the unidentified plant cutinase, causes cuticular defects in *Arabidopsis thaliana*. *Plant and Cell Physiology* 51:123–131
- [18] Dong X, Yi H, Han CT, Nou IS, Hur Y. 2016. GDSL esterase/lipase genes in *Brassica rapa* L.: genome-wide identification and expression analysis. *Molecular Genetics and Genomics* 291:531–542
- [19] Rastogi L, Chaudhari AA, Sharma R, Pawar PA. 2022. *Arabidopsis* GELP7 functions as a plasma membrane-localized acetyl xylan esterase, and its overexpression improves saccharification efficiency. *Plant Molecular Biology* 109:781–797
- [20] Yan X, Wu X, Sun F, Nie H, Du X, et al. 2024. Cloning and functional study of AmGDSL1 in *Agropyron mongolicum*. *International Journal of Molecular Sciences* 25(17):9467
- [21] Xu LZ. 2024. Study on the regulation of lipaseDIGDSL57 during early somatic embryogenesis in *dimocarpus longan* Lou. Master's Thesis. Fujian Agriculture and Forestry University.
- [22] Cho NH, Kim EY, Park K, Lim CJ, Seo DH, et al. 2023. Cosuppression of AtGELP22 and AtGELP23, two ubiquitinated target proteins of RING E3 ligase AtAIRP5, increases tolerance to drought stress in *Arabidopsis*. *Plant Molecular Biology* 112:357–371
- [23] Hao XY, Cai YZ, Yuan HL, Li R, Wang F, et al. 2014. Overexpression of a cotton GDSL lipase increases the oil content of *Brassica napus* L. *Journal of the Chinese Cereals and Oils Association* 29:63–73
- [24] Liu YJ, Guo DN, Zang Y, Tan XM, Li HM, et al. 2017. Identification and sequence analysis of GDSL esterase/lipase genes in Shatian pomelo. *Jiangsu Agricultural Sciences* 45:45–48 (in Chinese)
- [25] Ji ZR. 2024. Molecular mechanism of apple lipase MdGELP1 in inhibiting the infection of *colletotrichum gloeosporioides*. PhD. Thesis. Gansu Agricultural University. doi: 10.27025/d.cnki.ggsnu.2024.000016
- [26] Zhang YL, You CX, Li YY, Hao YJ. 2020. Advances in biosynthesis, regulation, and function of apple cuticular wax. *Frontiers in Plant Science* 11:1165
- [27] Chen C, Chen H, Zhang Y, Thomas HR, Frank MH, et al. 2020. TBtools: an integrative toolkit developed for interactive analyses of big biological data. *Molecular Plant* 13:1194–1202
- [28] Muralidharan M, Buss K, Larrimore KE, Segerson NA, Kannan L, et al. 2013. The *Arabidopsis thaliana* ortholog of a purported maize cholinesterase gene encodes a GDSL-lipase. *Plant Molecular Biology* 81:565–576
- [29] Zhang WJ, Zhou Y, Zhang Y, Su YH, Xu T. 2023. Protein phosphorylation: a molecular switch in plant signaling. *Cell Reports* 42:112729
- [30] Zhao T, Schranz ME. 2017. Network approaches for plant phylogenomic synteny analysis. *Current Opinion in Plant Biology* 36:129–134
- [31] Feng ZQ, Wang X, Li T, Wang XF, Li HF, et al. 2022. Genome-wide identification and comparative analysis of genes encoding AAPs in apple (*Malus × domestica* Borkh). *Gene* 832:146558
- [32] Ma Q, Su C, Dong CH. 2021. Genome-wide transcriptomic and proteomic exploration of molecular regulations in quinoa responses to ethylene and salt stress. *Plants* 10(11):2281
- [33] Mayfield JA, Preuss D. 2000. Rapid initiation of *Arabidopsis* pollination requires the oleosin-domain protein GRP17. *Nature Cell Biology* 2:128–130
- [34] Shen G, Sun W, Chen Z, Shi L, Hong J, et al. 2022. Plant GDSL esterases/lipases: evolutionary, physiological and molecular functions in plant development. *Plants* 11(4):468
- [35] Ling H. 2008. Sequence analysis of GDSL lipase gene family in *Arabidopsis thaliana*. *Pakistan Journal of Biological Sciences* 11:763–767
- [36] Cenci A, Concepción-Hernández M, Guignon V, Angenon G, Rouard M. 2022. Genome-Wide Classification and Phylogenetic Analyses of the GDSL-type esterase/lipase (GELP) family in flowering plants. *International Journal of Molecular Sciences* 23(20):12114
- [37] Park JJ, Jin P, Yoon J, Yang JI, Jeong HJ, et al. 2010. Mutation in *Wilted Dwarf* and *Lethal 1 (WDL1)* causes abnormal cuticle formation and rapid water loss in rice. *Plant Molecular Biology* 74:91–103
- [38] Xu G, Guo C, Shan H, Kong H. 2012. Divergence of duplicate genes in exon-intron structure. *Proceedings of the National Academy of Sciences of the United States of America* 109:1187–1192
- [39] Wong JJ, Au AYM, Ritchie W, Rasko JEJ. 2016. Intron retention in mRNA: no longer nonsense: known and putative roles of intron retention in normal and disease biology. *BioEssays* 38:41–49
- [40] Bataillon T, Gauthier P, Villesen P, Santoni S, Thompson JD, et al. 2022. From genotype to phenotype: genetic redundancy and the maintenance of an adaptive polymorphism in the context of high gene flow. *Evolution Letters* 6:189–202
- [41] Cannon SB, Mitra A, Baumgarten A, Young ND, May G. 2004. The roles of segmental and tandem gene duplication in the evolution of large gene families in *Arabidopsis thaliana*. *BMC Plant Biology* 4:10
- [42] Yu J, Wang J, Lin W, Li S, Li H, et al. 2005. The genomes of *Oryza sativa*: a history of duplications. *PLoS Biology* 3:e38
- [43] Jiao Y, Zhang J, Pan C. 2022. Genome-wide analysis of the GDSL genes in pecan (*Carya illinoensis* K. Koch): phylogeny, structure, promoter cis-elements, co-expression networks, and response to salt stresses. *Genes* 13(7):1103
- [44] Ursache R, De Jesus Vieira Teixeira C, Déneraud Tendon V, Gully K, De Bellis D, et al. 2021. GDSL-domain proteins have key roles in suberin polymerization and degradation. *Nature Plants* 7:353–364
- [45] Ling H, Zhao J, Zuo K, Qiu C, Yao H, et al. 2006. Isolation and expression analysis of a GDSL-like lipase gene from *Brassica napus* L. *BMB Reports* 39:297–303
- [46] Schlueter JA, Lin JY, Schlueter SD, Vasylenko-Sanders IF, Deshpande S, et al. 2007. Gene duplication and paleopolyploidy in soybean and the implications for whole genome sequencing. *BMC Genomics* 8:330
- [47] Yu X, Zhang W, Zhang Y, Zhang X, Lang D, et al. 2019. The roles of methyl jasmonate to stress in plants. *Functional Plant Biology* 46:197–212
- [48] Ding F, Wang X, Li Z, Wang M. 2022. Jasmonate positively regulates cold tolerance by promoting ABA biosynthesis in tomato. *Plants* 12(1):60



Copyright: © 2026 by the author(s). Published by Maximum Academic Press, Fayetteville, GA. This article is an open access article distributed under Creative Commons Attribution License (CC BY 4.0), visit <https://creativecommons.org/licenses/by/4.0/>.